

Comparison of Polyanilines Doped by Lignosulfonates with Three Different Ions

Jin-Qiao Dong, Qing Shen

State Key Laboratory for Modification of Chemical Fiber and Polymers, Polymer Department of Donghua University, 201620 Shanghai, People's Republic of China

Received 7 August 2011; accepted 1 December 2011

DOI 10.1002/app.36662

Published online in Wiley Online Library (wileyonlinelibrary.com).

ABSTRACT: Polyaniline (PANI) doped by three lignosulfonates (LGSs) with ions of sodium, calcium, and magnesium, respectively, was fabricated and compared. Results showed that the conductivity, solubility, and thermal stability of all these three LGSs-doped PANIs were enhanced, especially the LGS-Ca-doped PANI, when compared with the pure PANI. XRD, UV, and FTIR spectra indicated that the PANI doped by LGS-Ca facilitated electron delocalization, which enhances crystallization of PANI/LGS-Ca with

respect to the other two LGSs-doped PANIs. The PANI/LGS-Ca has the best thermal behavior with respect to the other two LGSs-doped PANIs due probably to the hydrogen bonding between LGS-Ca and PANI stable than that between the other two LGSs and PANI. © 2012 Wiley Periodicals, Inc. *J Appl Polym Sci* 000: 000–000, 2012

Key words: polyaniline; lignosulfonate; dopant; emulsifier; emulsion polymerization

INTRODUCTION

Polyaniline (PANI) is one of the most important conducting polymer and has been broadly studied and applied.^{1–14} Because PANI has some problems in application, e.g., insolubility and infusibility, these lead a lot of novel methods being developed.¹⁵ Additionally, considering lignosulfonate (LGS) is a water-soluble surfactant^{16–19}; several researchers have applied LGS to dope PANI and obtained positive results.^{20–22} Different than reported case on using LGS to dope PANI, recently, we have applied LGS to modify carbon nanotubes, CNTs, initially then applied the LGS-modified CNTs to dope PANI obtained good results.¹⁵

Although the use of LGS to dope PANI has been broadly reported elsewhere,^{20–22} it should be addressed that the commercial LGS is usually with different cations, e.g., Na⁺, Ca²⁺, and Mg²⁺, and yet the difference on use of these different ions-based LGSs to dope PANI is unknown. In fact, recently we have studied these LGSs and found these LGSs have different surface properties.²³ Thus, it is probably to assume that the PANI if being doped by these different ions-based LGSs may have different properties.

Therefore, the aim of this work is to compare several PANIs doped by LGS-Na, LGS-Ca, and LGS-Mg, respectively. We characterized and compared the

structure and properties, e.g., the conductivity, solubility, and thermal stability, of these LGSs-doped PANIs.

EXPERIMENTAL

Materials

The aniline (ANI), ammonium peroxodisulfate (APS), and the solvents in analytical grade reagents were used as received, and all of them were obtained from the Sinopharm Chemical Reagent Co., Ltd. located at Shanghai, China.¹⁵

Three LGSs, e.g., LGS-Na, LGS-Mg, and LGS-Ca, from Jiangmen Sugar Cane Chemical Factory, Guangdong, China were used as received. These LGSs have been recently introduced detailed.²³

Distilled water was laboratory made and always used in this work.

Preparation of LGS-doped PANI

Initially, 0.935 g LGS was dissolved in 100 mL 0.01M HCl solution in the presence of isooctane, then 4.65 mL (0.05 mol) ANI was added to start the emulsion polymerization. Under an ultrasonic condition for 10–15 min, a micellar solution was formed. In addition, an oxidizing agent solution was prepared by dissolving 11.41 g (0.05 mol) APS in 50 mL distilled water and applied gradually to add (about 30 min) to the ANI solution to avoid the reaction mixture overheated. The polymerization temperature was kept at 5°C, and the whole reaction time was controlled about 24 h.

Correspondence to: Q. Shen (sqing@dhu.edu.cn).

TABLE I
A Comparison of the Elemental Analyses of PANI/LGSs and PANI Obtained from Emulsion Polymerization

Samples	C (%)	N (%)	S (%)	C/N (mol/mol)	Conductivity (S/cm)
PANI	53.74	10.32	0.405	6.08	1.283×10^{-4}
PANI/LGS-Na	56.34	6.521	4.481	10.08	2.408×10^{-2}
PANI/LGS-Mg	55.78	6.754	3.814	9.64	1.605×10^{-2}
PANI/LGS-Ca	57.45	5.931	4.742	11.30	5.482×10^{-2}

The polymerization was terminated by pouring about 500 mL acetone into the emulsion to cause the precipitation of the PANI/LGS complex. As observed, this product presented dark green. The obtained PANI/LGS powders were filtered and washed three times using 300 mL acetone and 300 mL distilled water, respectively. All samples were finally dried by a vacuum oven at 50°C for 24 h.

A LGS-free PANI was also prepared as the same as above and taken as a reference.

Characterizations

The elemental of C, H, S, and N of PANI/LGSs were analyzed by Vario EL III instrument (elementar Analysensysteme GMBH, Germany).¹⁵

UV-vis spectra of PANI/LGSs were recorded in the wavelength range of 190–800 nm at room temperature, 25°C, using Lambda 35 UV-vis spectrometer (Perkin Elmer, USA). Each PANI/LGS was dissolved in DMSO under the ultrasonication condition.¹⁵

The FTIR spectra of PANI/LGSs were recorded using NEXUS 8700 (Nicolet, UK) in the range of 400–4000 cm^{-1} with the resolution of 4 cm^{-1} . The KBr pellet technique was adopted to prepare all samples.^{15,23}

The electrical conductivity of PANI/LGSs was measured using SDY-4 Four-Point Probe Meter (Four Dimensions, Inc. USA) at 25°C. The pellets were prepared by subjecting the powder sample to a pressure of 30 MPa, and the reproducibility was checked by measuring the resistance of each pellet three times.¹⁵

The X-ray diffraction (XRD) curves of these PANI/LGSs were recorded by the Rigaku D/Max-2550 PC instrument (Rigaku, USA) at 40 kV, 30 mA, by the Cu-K α monochromatic radiation with a wavelength of 1.5406 Å, after scanning in the 2 θ range of 3–60° at intervals of 0.02.¹⁵

The thermal stability of all PANI samples were characterized by the NETZSCH STA-409PC (NETZSCH, Germany) from 25 to 850°C with a heating rate of 10°C/min under N₂ atmosphere.¹⁵

RESULTS AND DISCUSSION

The effect of LGSs with different ions on the conductivity of doped PANI is summarized in Table I.

Comparing to the referenced PANI, it was found that the conductivity of all LGS-doped PANIs is increased, especially the LGS-Ca doped PANI, and all these samples following the conductivity order as: PANI/LGS-Ca.PANI/LGS-Na.PANI/LGS-Mg.PANI. The reason on the conductivity increase for LGS-doped PANI is because the twice roles of LGS, e.g., a dopant and an emulsifier, to synchronously cause the π - π^* interactions taking place between the surface of LGS and the quinoid ring of PANI which improving the degree of electron delocalization.^{20–22} Thus, the chains of LGSs-doped PANIs were reoriented to lead the crystallinity of PANI enhanced. Because the PANI/LGS-Ca presented a higher conductivity when compared with other two LGSs-doped PANIs (Table I), it is also considered that this provides a possibility for production of PANI with adjustable conductivity. Because the LGS-Ca has a greater surface free energy than that of the LGS-Mg and LGS-Na,^{20–22} it is assumed that the PANI/LGS-Ca may have higher surface activity when compared with other two LGS-doped PANI. In fact, we found that above presented conductivity order is the same as the Lifshitz-van der Waals component of these LGSs.²³ This proven that the LGS as a template took a conformation with more extended chains than pure PANI, leading to an increased conjugation length, thus enhancing the conductivity of LGS-PANI owing to the free motion of charge carriers.²²

The doping of LGS in PANI is also proven by elemental analysis as showed in Table I. Taking the C/N ratio as a measure, we compare these PANI samples and found that all LGS-doped PANIs have higher C/N ratio values than the pure PANI. Furthermore, we found that the S element was increased in all LGS-doped PANIs when compared with the LGS-free PANI, suggesting the SO₃⁻ group of LGS doped in PANI.

The UV spectra of all PANIs were showed in Figure 1. Of which, three main UV bands are typically for PANI which are located at the areas of 340–360, 580–600, and 690–700 nm corresponding to the π - π^* transition of ring,¹⁵ the excision transition for higher energy occupied benzenoid moiety to lower energy unoccupied quinoid moiety, and the polaron transitions,²⁴ respectively. The effects from LGSs on PANI are found in 340–360 and 690–700 nm ranges, respectively, because the peak in the

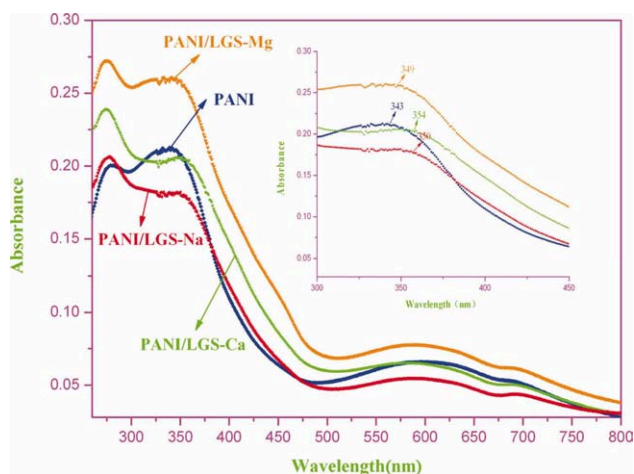


Figure 1 UV-vis spectra of three PANI/LGSs and referenced PANI obtained by emulsion polymerization. [Color figure can be viewed in the online issue, which is available at wileyonlinelibrary.com.]

first range was shifted from 343 upward to 354 nm for PANI/LGS-Ca, to 350 nm for PANI/LGS-Na, and to 349 nm for PANI/LGS-Mg, respectively (Fig. 1), and in the second range, the peak was shifted for all these LGSs-doped PANIs. Obviously, these UV evidences support above conclusion to indicate the doping of LGS in PANI facilitated the electron delocalization. Thus, it is furthermore known that the doping-induced interactions between the chains of PANI and LGS are stronger in PANI/LGS-Ca and weaker in other two PANI/LGSs.

The FTIR spectra of all PANIs were showed and compared in Figure 2. Three LGS-doped PANIs presented main bands at 3440 cm^{-1} corresponding to the N-H stretching mode, 2922 cm^{-1} due to the C-H stretching, 1580 cm^{-1} due to oxidation of PANI/LGS, 1480 cm^{-1} due to the emeraldine salts benzenoid,^{24–26} 1300 cm^{-1} due to the contribution of the C-N stretching of benzenoid unit,²⁵ and 800 cm^{-1} due to the 1,4-disubstituted aromatics of PANI and PANI/LGS.¹ Because several new peaks located at 3227 , 3236 , and 3228 cm^{-1} all due to the O-H stretching in LGS-doped PANIs (Fig. 2), this proven that the doping of LGS into PANI chains is also rely on the O-H groups. Because LGS has the O-H stretching at 3420 cm^{-1} ,²³ its shift in PANI/LGS is, therefore, a reasonable measure on understanding of the hydrogen bond formation. In Figure 2, the synthesis of PANI in the presence of the LGS is assumed, wherein the LGS is a template where the SO_3^- groups of LGS doped in PANI are the peaks of 512 , 586 , 589 , and 590 cm^{-1} .^{25,27} The peak appeared at 1124 cm^{-1} due to the N=Q=N stretching is typically identified as the “electron-like band” for characterizing of PANI,²⁶ in relation to the electrons delocalization.^{27–29} In terms of this peak (1124 cm^{-1}), therefore, its shift at 1140 cm^{-1} for

PANI/LGS-Ca and shifted at 1134 cm^{-1} for PANI/LGS-Na, respectively (Fig. 2), could be applied to deduce a related mechanism on LGS doping of PANI as described in Figure 3.

The wide-angle XRD curves of all LGS-doped PANIs and referenced PANI were presented in Figure 4. We found that the pure PANI appeared two typical 2θ peaks at 19.45 and 25.07° represent the reflection plane of (020) and (200) because of the periodicity parallel and perpendicular to the polymer chains, respectively,³⁰ and the peak at $2\theta = 25.07^\circ$ is intensely than that of the peak at $2\theta = 19.45^\circ$, in good agreement with literature reported PANI after doping.^{31,32} Thus, we take these two peaks to compare the LGS-doped PANIs. As Figure 4 showed that these two peaks are shifted, e.g., for PANI/LGS-Ca upward to at 19.57 and 25.19° , for PANI/LGS-Na upward to at 19.83 and 25.42° , and for PANI/LGS-Mg one on the contrary to locate at 19.33 and another remained at the same position at 25.07° , respectively. These findings are of interest and clearly indicated that the doping of LGSs in PANI caused the structure change, and it is mainly in the improving the crystalline order and the degree of crystallinity.^{20–22} However, this is controlled by the LGS type. This suggests that we can apply these LGSs to control the PANI structure. In fact, above mentioned peak shift could be understood. For example, the PANI/LGS-Na presented a peak shift from 25.07 to 25.42° is due to the narrower interval among lattices of PANI/LGS-Na. In contrast to the pure PANI, we also found a new peak appeared at $2\theta = 6.46$ and 8.33° for PANI/LGS-Ca and PANI/LGS-Na, and a new peak appeared at $2\theta = 16.23^\circ$ uniquely for PANI/LGS-Ca

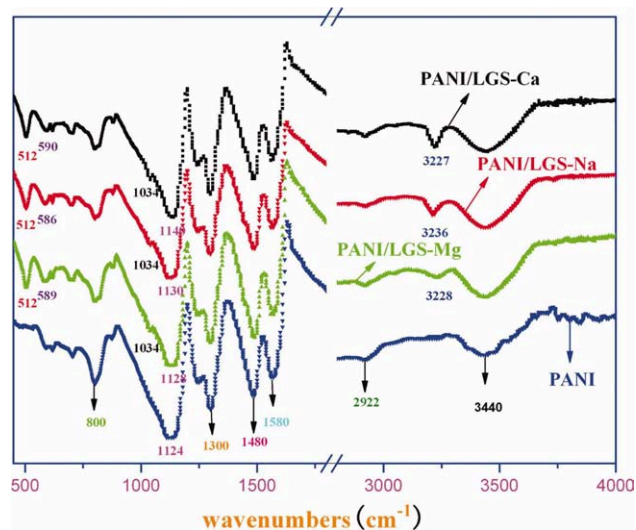


Figure 2 FT-IR spectra of three PANI/LGSs and referenced PANI obtained by emulsion polymerization. [Color figure can be viewed in the online issue, which is available at wileyonlinelibrary.com.]

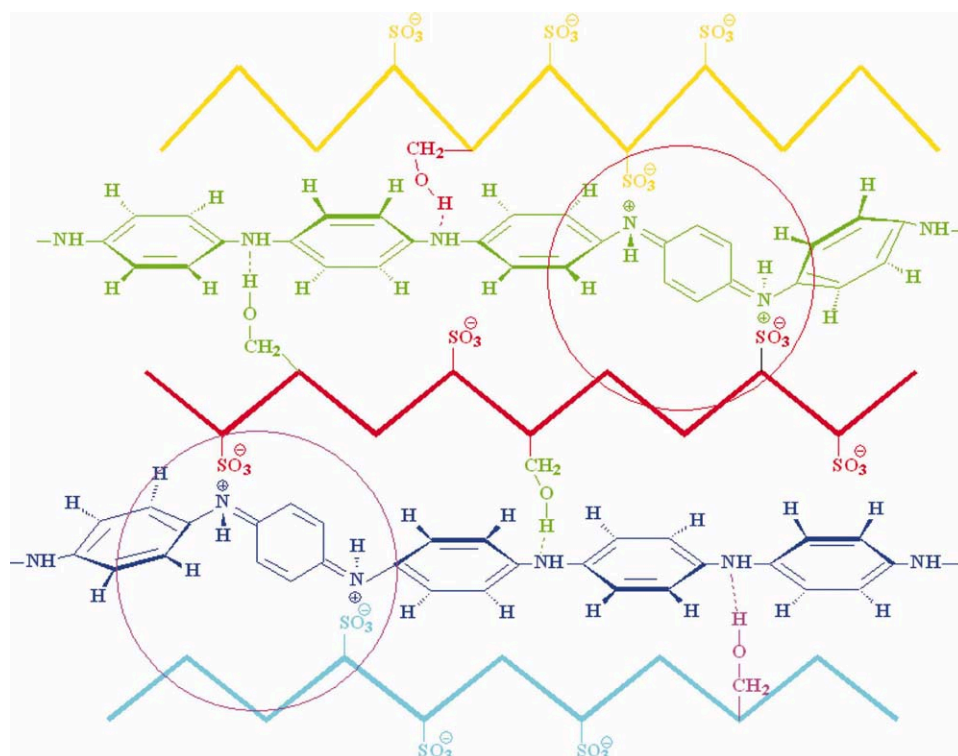


Figure 3 Scheme on H-bonds formation in PANI/LGS during the doping of LGS in PANI by emulsion polymerization. [Color figure can be viewed in the online issue, which is available at wileyonlinelibrary.com.]

(Fig. 4), respectively. All these phenomena again indicated that the PANI structure was highly ordered after doping of LGS and the degree is, however, to vary dependence of the LGS type. In above mentioned new evidences, the new peak appeared at $2\theta = 6.46^\circ$ arises from the LGS-doped PANI is capably explained to the interdigitations and crystallization of the side chains of the comb-shaped PANI. In addition, the peaks located at $2\theta = 19.57$ and 25.19° are stronger for PANI/LGS-Ca and weaker for other two LGS-based PANIs indicating the doping of LGS-Ca in PANI caused the structure of PANI/LGS-Ca reordered well than that of the other two LGSs-doped PANIs.

Table II summarized the crystalline values of these PANI/LGSs, where the PANI/LGS-Ca showed higher value than that of the pure PANI to support above explanation. Based on these values and above assumption, thus, a related scheme was described in Figure 5, which claimed that the space orientation to be occurred in PANI/LGS due to the PANI chains planar aligned by the doped LGS chains through emulsion polymerization, and the chains of both PANI and LGS to be alternatively to rearrange under the electrostatic force and hydrogen bonding. However, it should be addressed that above mentioned chain behaviors are reasonably in different because it dependence of the LGS types. Because LGS-Ca has been known to have the highest surface

free energy than other two LGSs,²³ this LGS-doped PANI causes the structure of PANI compacted and reordered well when compared with other two LGSs-doped PANIs, indicating the LGS-Ca-based emulsion to be activity for PANI molecules growth.

With respect to the fact that LGS-Ca having the higher surface energy than other two LGSs²³ and

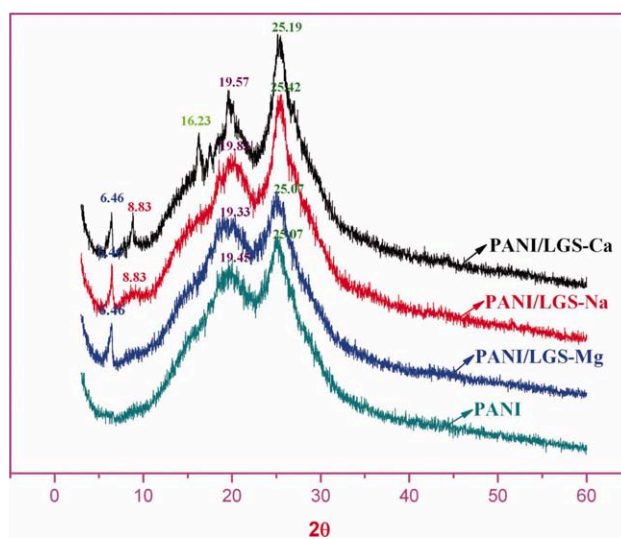


Figure 4 WAXD patterns of three PANI/LGSs and referenced PANI obtained by emulsion polymerization. [Color figure can be viewed in the online issue, which is available at wileyonlinelibrary.com.]

TABLE II
Parameters from WAXD Patterns of PANI/LGSs and PANI Obtained from Emulsion Polymerization

	PANI	PANI/ LGS-Ca	PANI/ LGS-Na	PANI/ LGS-Mg
Center of peak position	19.45°	6.46°	6.46°	6.46°
	25.07°	8.33°	8.33°	19.33°
		19.57°	19.83°	25.07°
Full width at half maximum	0.734	0.363	0.365	0.392
	0.968	0.431	0.743	0.645
		0.610	0.626	0.912
		0.557	0.868	
		0.805		
Crystallinity	32.62%	40.02%	38.11%	34.62%

this LGS-doped PANI presented better conductivity indeed (Table I), its solubility behavior is a new interest. Taking several organic solvents as probes, the solubility of these PANIs were summarized and compared in Table III. As expected, a comparison of these data showed that the PANI/LGS-Ca presented well dissolution behavior, especially in NMP. This further proven that the strong polarity group, SO_3^- , of LGS was doped in PANI chains and to further suggest that the polarity of PANI was enhanced by doping of LGS, especially the LGS-Ca. In Table III, it is also noted that the LGS-doped PANI is unable to dissolve in xylene, acetone, and propylene carbonate. The reason is considered perhaps due to the surface properties of these solvents and requiring the furthermore investigation.

The thermal stability of these three LGS-doped PANIs was examined by TGA and presented in Figure 6. Noted in the first heating step when the temperature was increased from 30 to 128°C, a small weight loss was occurred for all LGS-doped PANIs due to the moisture expulsion from the samples.³³ In the second step when the temperature was further more increased from 185 to 385°C, the weight loss

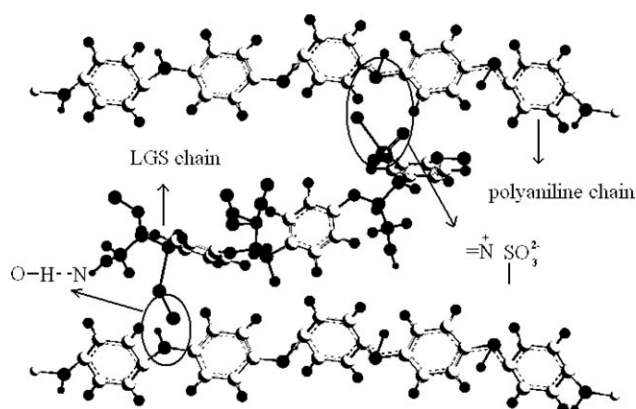


Figure 5 Scheme on the space orientation of PANI/LGS.

TABLE III
The Solubility of PANI/LGS-Ca in Different Solvents

Solvents	Dielectric constant	Solubility parameter	Solubility
NMP	32.2	23.1	+++
DMSO	47.2	24.6	+++
DMF	38.2	24.8	+++
Methyl ethyl ketone	18.6	19	++
Hexane	1.9	14.9	++
Chloroform	4.8	19	+
Butylacetate	5.1	17.4	+
4-Methyl-2-pentanone	13.1	17.2	+
Acetone	21	20.3	×
Propylene carbonate	–	27.2	×
Xylene	2.4	18	×
Water	80.1	47.9	×

×, +, ++, and +++ represent the solubility (g/100 mL) <0.5, <2, <6, and <12, respectively.

was prolonged due to the unbounded LGS and other oligomers removed. In this step, the degradation was appeared at 310.7°C for PANI/LGS-Ca, which was higher than the pure PANI, e.g., at 260.8°C. This implies that the LGS-Ca-doped PANI is homogeneously to support the conclusions of our above XRD, FT-IR, and elemental analysis. In Figure 6, a significant weight loss was found at the third and fourth steps corresponding to the temperature ranges in 443–605°C and 615–845°C, respectively, because all these PANI/LGSs presented weight loss. This is probably due to the bounded dopant and oxidative decomposed.³⁴ In these steps, the de-dope of PANI/LGS-Mg seems to be extremely fast as seeming it started since 557°C, and this is also occurred for pure PANI. This suggests that the LGS-Mg-doped PANI is worse than that of LGS-Ca- and LGS-Na-doped PANIs. The derivative thermograms

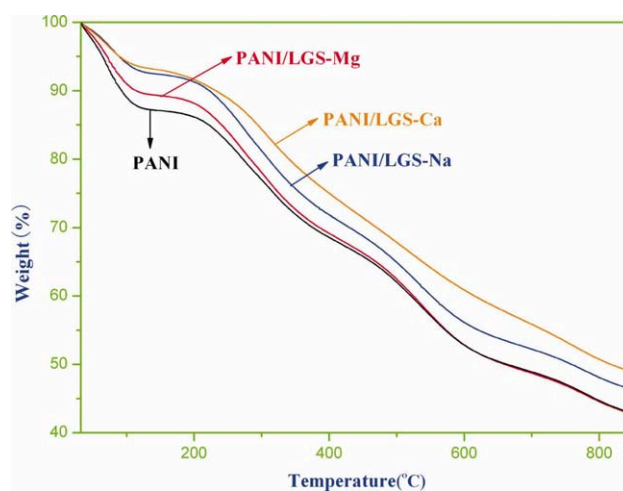


Figure 6 TG curves of three PANI/LGSs and referenced PANI obtained by emulsion polymerization. [Color figure can be viewed in the online issue, which is available at www.interscience.wiley.com.]

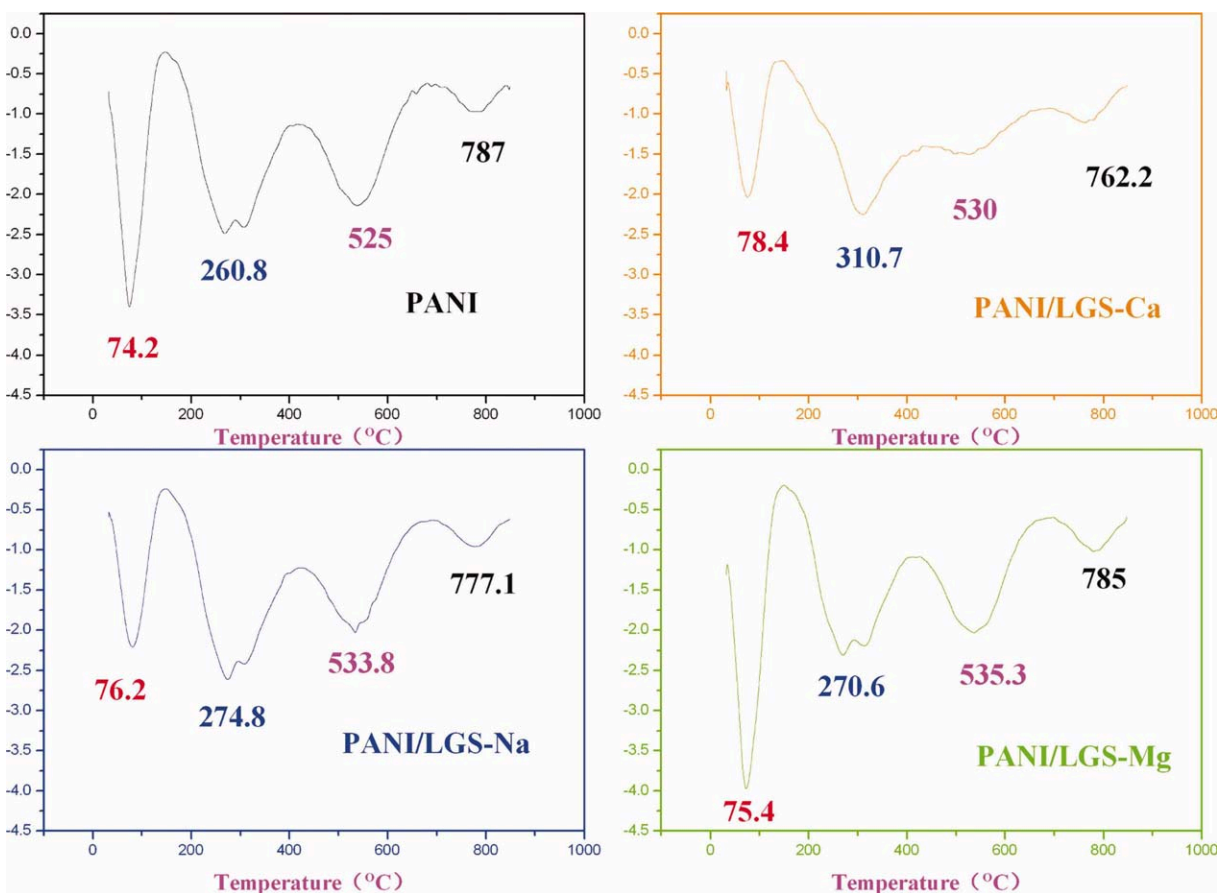


Figure 7 DTG curves of three PANI/LGSs and referenced PANI obtained by emulsion polymerization. [Color figure can be viewed in the online issue, which is available at wileyonlinelibrary.com.]

of three PANI/LGSs were furthermore shown in Figure 7, and the comparison of LGS-doped PANIs with the pure PANI indicated that the weight lost is faster for PANI and slowly for all LGS-doped PANIs, especially for PANI/LGS-Ca. These thermal behaviors are expected and again indicated that the LGS-Ca-doped PANI has the best thermal behavior than that of other two LGSs-doped PANIs. On the basis of this finding, it is also considered that the hydrogen bonding between LGS-Ca and PANI might be stable than that of the other two LGSs-doped PANIs.

CONCLUSIONS

The doping of LGSs with different ions in PANI by emulsion polymerization has been experimentally investigated and compared. Results showed the doping of LGS-Ca, LGS-Mg, and LGS-Na all enhanced the conductivity, solubility, and thermal stability of PANI, while the best is the doping of LGS-Ca. The reason is explained due to the LGS-Ca having higher surface free energy than that of the other two LGSs, which is thus benefit facilitating the electron delocalization for PANI to lead the PANI to enhance its crystallization.

References

1. Palaniappan, S.; John, A. *Prog Polym Sci* 2008, 33, 732.
2. Gospodinova, N.; Terlemezyan, L. *Prog Polym Sci* 1998, 23, 1443.
3. Patil, A. O.; Heeger, A. J.; Wud, F. *Chem Rev* 1988, 88, 183.
4. Huang, W. S.; Humphrey, B. D.; MacDiarmid, A. G. *J Chem Soc Faraday Trans* 1986, 82, 2385.
5. Yeh, J. M.; Liou, S. J.; Lai, C. Y.; Wu, P. C.; Tsai, T. Y. *Chem Mater* 2001, 13, 1131.
6. Epstein, A. J.; Ginder, J. M.; Zuo, F.; Bigelow, R. W.; Woo, H. S.; Tanner, D. B.; Richter, A. F.; Huang, W. S.; MacDiarmid, A. G. *Synth Mater* 1987, 18, 303.
7. MacDiarmid, A. G.; Epstein, A. J. *Faraday Discuss Chem Soc* 1989, 88, 317.
8. Urbach, B.; Korbakov, N.; Bar-David, Y.; Yitzchaik, S.; Saar, A. *J Phys Chem C* 2007, 111, 16586.
9. Harlev, E.; Gulakhmedova, T.; Rubinovich, I.; Aizenshtein, G. *Adv Mater* 1996, 8, 994.
10. Krishna, M. V. B.; Karunasagar, D.; Rao, S. V.; Arunachalam, J. *Talanta* 2005, 68, 329.
11. Anderson, M. R.; Mattes, B. R.; Reiss, H.; Kaner, R. B. *Science* 1991, 252, 1412.
12. Kaner, R. B. *Synth Mater* 2001, 125, 65.
13. Xue, H. G.; Shen, Z. Q. *Talanta* 2002, 57, 289.
14. Kotwal, A.; Schmidt, C. E. *Biomaterials* 2001, 22, 1055.
15. Dong, J. Q.; Shen, Q. *J Polym Sci B* 2009, 47, 2036.
16. Dawy, M.; Shabaka, A. A. A.; Nada, A. M. A. *Polym Degrad Stab* 1998, 62, 455.
17. Chen, R. L.; Kokta, B. V.; Daneault, C. *J Polym Sci* 1986, 32, 4815.

18. Alexi, P.; Kosikova, B.; Podstranska, G. *Polymer* 2000, 41, 4901.
19. Fredheim, G. E.; Christensen, C.; Bjørn, E. *Biomacromolecules* 2003, 4, 232.
20. Roy, S.; Fortier, J. M.; Nagarajan, R.; Tripathy, S.; Kumar, J.; Samuelson, L. A.; Bruno, F. F. *Biomacromolecules* 2002, 3, 937.
21. Taylor, K. K.; Cole, C. V.; Soora, R.; Dilday, J. C.; Hill, A. M.; Berry, B.; Viswanathan, T. *J Appl Polym Sci* 2008, 108, 1496.
22. Shao, L.; Qiu, J. H.; Feng, H. X.; Liu, M. Z.; Zhang, G. H.; An, J. B.; Gao, C. M.; Liu, H. L. *Synth Met* 2009, 159, 1761.
23. Shen, Q.; Zhang, T.; Zhu, M. F. *Colloids Surf A* 2008, 320, 57.
24. Kim, Y. H.; Foster, C.; Chiang, J.; Heeger, A. J. *Synth Mater* 1989, 29, 285.
25. Gopalan, A. I.; Lee, K. P.; Santhosh, P.; Kim, K. S.; Nho, Y. C. *Comp Sci Tech* 2007, 67, 900.
26. Quillard, S.; Louarn, G.; Lefrant, S.; MacDiarmid, A. G. *Phys Rev B* 1994, 50, 12496.
27. Jeevananda, T.; Siddaramaiah, H. K.; Nam, B. H.; Seok, H.; Joong, L. *Polym Adv Technol* 2008, 10, 1002.
28. Kang, E. T.; Noeh, K. G.; Tan, K. L. *Prog Polym Sci* 1998, 23, 277.
29. Lee, D.; Char, K.; Lee, S. W.; Park, Y. W. *J Mater Chem* 2003, 13, 2942.
30. Moon, Y. B.; Cao, Y.; Smith, P.; Heeger, A. J. *Polym Commun* 1989, 30, 196.
31. Pouget, J. P.; Jozefowicz, M. E.; Epstein, A. J.; Tang, X.; MacDiarmid, A. G. *Macromolecules* 1991, 24, 779.
32. Grulke, E. A. In: *Polymer Handbook*, 3rd, ed.; Brandrup, J., Immergut, E. H., Eds.; Wiley: New York, 1989; p 519.
33. Jeevananda, T.; Siddaramaiah, S.; Seetharamu, S.; Saravanan, L.; Souza, D. *Synth Mater* 2004, 140, 247.
34. Shaffer, S. P.; Windle, A. H. *Adv Mater* 1999, 11, 937.